

## Numerical Simulation of Sound Propagation Through Time-Dependent Random Media

D. Juvé, Ph. Blanc-Benon, and K. Wert

Laboratoire de Mécanique des Fluides et d'Acoustique,

U.M.R. C.N.R.S. 5509, Ecole Centrale de Lyon,

B.P. 163, 69131 Ecully Cedex, France

*The propagation of acoustic waves through spatially random, time-independent media has been extensively studied in recent years using a direct simulation approach. In this paper we present an extension of this technique to media that slowly evolve in time. A "classical" parabolic equation is used for computing the acoustic field, but with time-dependent coefficients determined either by a fluid dynamics code (Large Eddy Simulation) or with time-dependent Random Fourier Modes.*

### 1 Introduction

An acoustic wave propagating through a turbulent atmosphere is significantly affected by the variation in the value of the refractive index along the propagation path. The influence of temperature and wind velocity fluctuations has been demonstrated in many experimental studies. In recent years several authors have taken into account the effect of turbulence on sound propagation through numerical simulations for realistic cases. As an example, for sound propagation over long distances when strong negative vertical sound-speed gradients refract sound upward, it has been confirmed that the increase of the mean sound-pressure level in the shadow zone is due to the scattering of sound by turbulence. Currently, the numerical simulations are based on a parabolic equation with a random-in-space-but-static index of refraction (frozen turbulence hypothesis). In this paper we describe some possible extensions of the previous analyses to take into account the (slow) evolution in time of the propagation medium.

This paper is organized as follows. In section 2 we describe the method used to compute sound propagation through a random medium, modelled as a series of static, independent realizations. In section 3 we give typical results obtained with this technique for atmospheric propagation. Section 4 presents the extension of the method to slowly varying time-dependent turbulence. Results are given for two different methods of generating the evolving random field: Large Eddy Simulations, and Random Fourier Modes. The paper ends with a conclusion.

## 2 The "direct" numerical simulation of sound propagation through turbulence

The classical method of handling the propagation of waves through random media relies on a statistical approach. Starting from a parabolic approximation of the Helmholtz equation with a random refraction index, equations are deduced for the various statistical moments of the field: mean intensity, spatial coherence function, etc. However, to obtain equations in closed form, a priori hypotheses have to be made about the correlation of the field (delta-correlation along the mean direction of propagation). Furthermore, the theory has been essentially developed for an homogeneous deterministic medium on which random fluctuations are superimposed. No theoretical results are available when the deterministic part of the refraction index is varying with height or when reflections occur on an impedance surface, as is the case in sound propagation through the atmosphere. In recent years, a different approach has been developed to overcome these limitations (Gilbert *et al.*,<sup>7</sup> Juvé *et al.*<sup>8</sup>). A deterministic wave equation is solved for a series of realizations of a simulated turbulent field; statistical results are then obtained through ensemble averaging. In our group, we have developed a new strategy to construct the synthesized turbulent fields (Random Fourier Modes method); its main advantage is the possibility of easily generating vector (velocity) random fields in addition to scalar ones.<sup>2</sup> In most studies, the Helmholtz equation with random index of refraction is generally accepted:

$$\left[ \nabla^2 + k_0^2 (1 + 2\mu(\mathbf{x})) \right] p'(\mathbf{x}) = 0 \quad (1)$$

$$\mu(\mathbf{x}) = -\frac{u_x(\mathbf{x})}{c_0} - \frac{T'(\mathbf{x})}{2\bar{T}}. \quad (2)$$

where  $p'(\mathbf{x})$  denotes the spatial dependence of the pressure,  $k_0$  is the acoustic wave number and  $\mu(\mathbf{x})$  is the random part of the index of refraction, which is related to the fluctuation of the temperature  $T'$  and to the component  $u_1 = u_x$  of the velocity fluctuation in the direction of propagation  $x$ .  $c_0$  and  $\bar{T}$  are, respectively, the sound speed without turbulence and the mean temperature. The Helmholtz equation is then approximated by a parabolic, one-way equation solved through a marching algorithm. For example, the "standard" parabolic equation can be used. Assuming that the spatial dependence of the acoustic pressure has an envelope  $\Psi(x, \rho)$  slowly varying with  $x$ :

$$p'(\mathbf{x}) = p'(x, \rho) = \Psi(x, \rho) \exp(ik_0 x) \quad (3)$$

where  $\rho$  is the lateral distance. The Helmholtz equation is transformed into:

$$2ik_0 \frac{\partial}{\partial x} \Psi(x, \rho) + \Delta_\rho \Psi(x, \rho) + k_0^2 \frac{\mu}{2}(x, \rho) \Psi(x, \rho) = 0. \quad (4)$$

In practice more efficient, wide-angle equations are used, solved through finite difference or Fourier techniques. Results have been obtained in the case of a homogeneous deterministic background for the intensity fluctuations at one or two points, as well as the spatial transverse or longitudinal correlation function. Most of the computations have been conducted in 2D, but some limited results are also available for the 3D case (<sup>3</sup> and <sup>4</sup>). In the following section we describe some of the results obtained

along this line for atmospheric sound propagation.

### 3 Some examples of sound propagation through a random atmosphere

#### 3.1 Modelling of the random turbulent field

Here the medium is to be modelled by a sequence of independent realizations of a frozen random field. Following Kraichnan,<sup>15</sup> the velocity at a given point  $\mathbf{x}$  is simulated by the sum of a limited number  $N$  of incompressible random Fourier modes :

$$\mathbf{u}(\mathbf{x}) = \sum_{n=1}^N \tilde{\mathbf{u}}_n \cos[\mathbf{k}_n \cdot \mathbf{x} + \psi_n] \quad (5)$$

A similar expression is used for scalar fluctuations (temperature fluctuations for example):

$$T'(\mathbf{x}) = \sum_{n=1}^N \tilde{T}_n \cos[\mathbf{k}_n \cdot \mathbf{x} + \phi_n] \quad (6)$$

The direction of the wave vector  $\mathbf{k}_n$  and the phases  $\psi_n, \phi_n$  are independent random variables with uniform probability distributions, resulting in homogeneous, isotropic fields. The amplitude of each mode is considered to be a deterministic variable whose value is set according to the energy spectrum under consideration. The most used forms are the Gaussian-derived spectrum (corresponding to a Gaussian longitudinal correlation function), and the von Karman spectrum. Examples of simulated scalar fields are shown on Fig. 1

With the Gaussian spectrum, characterized by one single scale  $L$ , blobs of size roughly equal to  $L$  are clearly seen with smooth transition between hot and cold regions. In the case of the von Karman spectrum, characterized by an outer scale  $L_0$  (large eddies), an inner scale  $l_0$  (small eddies) and a significant inertial range between them (Kolmogorov -5/3 law), the behaviour is markedly different: The map displays both large and small structures; the boundaries between hot and cold zones are highly twisted and reminiscent of fractal curves. These differences in the spatial structure of the index of refraction have been shown to strongly influence the sound scattered by turbulence in shadow zones.<sup>11</sup>

#### 3.2 Sound propagation in an upward-refracting atmosphere

In this paragraph we present two types of results obtained using the approach described above and pertaining to the propagation of sound waves in an upward-refracting atmosphere. In such conditions, a deterministic shadow zone appears at short distance from a near-ground source. For a receiver located in this zone, there is no direct ray coming from the source, and energy can penetrate into the shadow only through diffraction effects. A deterministic parabolic equation computation shows that the predicted levels are well below measured values. When the random nature of the atmosphere is correctly taken into account, our simulations lead to a very good agreement with the experimental

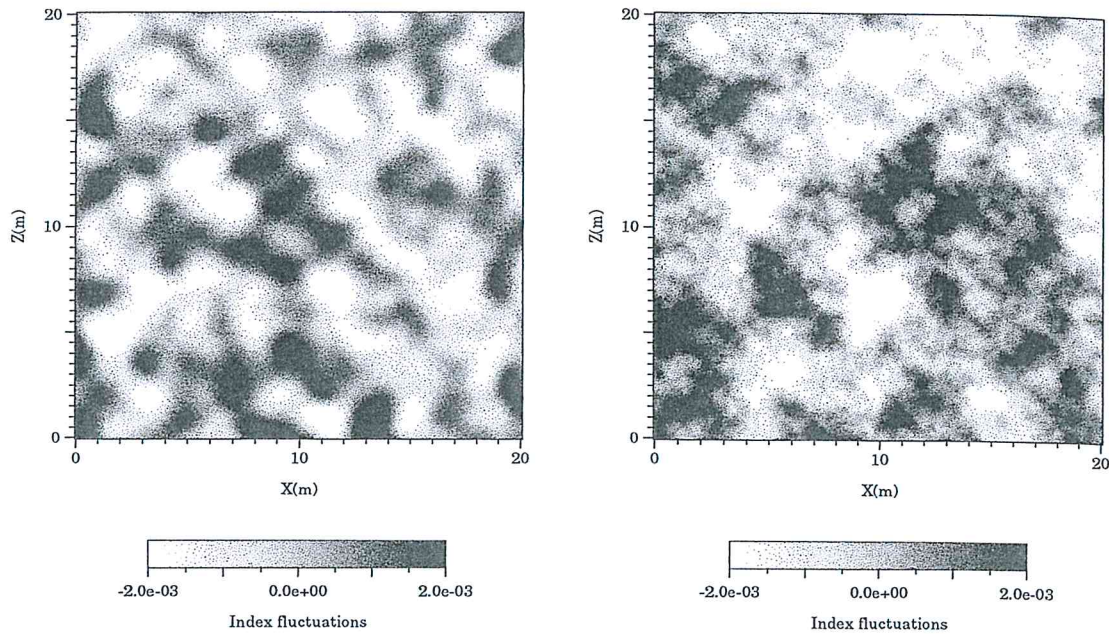


Figure 1: One realization of the refraction index field. The figure on the left is calculated using a Gaussian-derived spectrum, and the figure on the right is calculated using a von Karman spectrum.

data. This is illustrated on Fig. 2 for two values of the frequency and for "weak refraction" conditions (Wiener *et al*<sup>16</sup>).

Results for other refraction conditions and details of the computations are given in Chevret *et al.*<sup>6</sup> More complex acoustic quantities are also easily obtained with the direct simulation method. As an example, we consider in Fig. 3 the evolution of the normalized squared pressure amplitude computed for each of 600 realizations of the turbulent field. For a receiver located in the shadow zone, the squared pressure displays an intermittent evolution, with sporadic peaks of very high level (up to 100 times the mean value). The associated amplitude distribution is very far from a Gaussian (the classical distribution law in the region of small perturbations) and is well approximated by a Gamma distribution, see Fig. 4. Experimental studies<sup>(13)</sup> in the atmosphere have indeed demonstrated the intermittent character of the received sound amplitude in a shadow zone. It is then tempting to interpret the numerical results as a time series; but it must be remembered that every realization is independent from the other, and that the numerical results can only be interpreted on a statistical basis. To compare to the experimental work, we have developed a time-dependent numerical simulation, which we describe in the following section.

## 4 Simulation of sound propagation through time-dependent turbulence

### 4.1 Characteristic time scales

The usual static approach considers the turbulent field as frozen during the transit time of the acoustic wave. To relax this restrictive condition, we adopted an heuristic point of view. The strategy

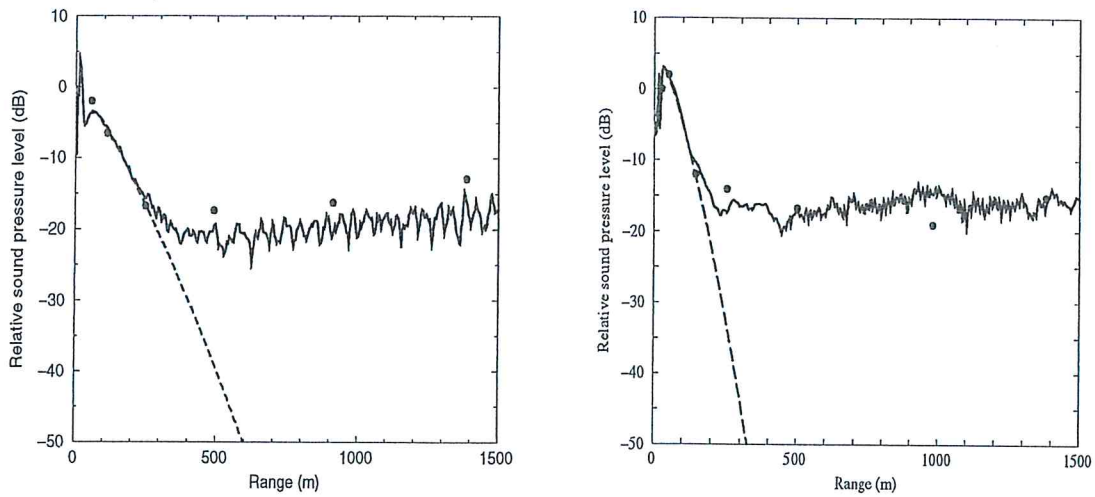


Figure 2: Relative sound pressure level: comparisons between the Wiener & Keast measurements ( $\bullet$ ), a deterministic calculation (---) and our model (—) ( $h_s = 3.7$  m,  $h_r = 1.5$  m,  $\sigma = 300000$  N $\times$ m $^{-4}$  $\times$ s,  $\langle\mu^2\rangle = 2 \times 10^{-6}$ ,  $L = 1.1$  m). The left-hand plot is for weak refractive conditions with  $f = 424$  Hz, the right-hand plot is for weak refractive conditions with  $f = 848$  Hz.

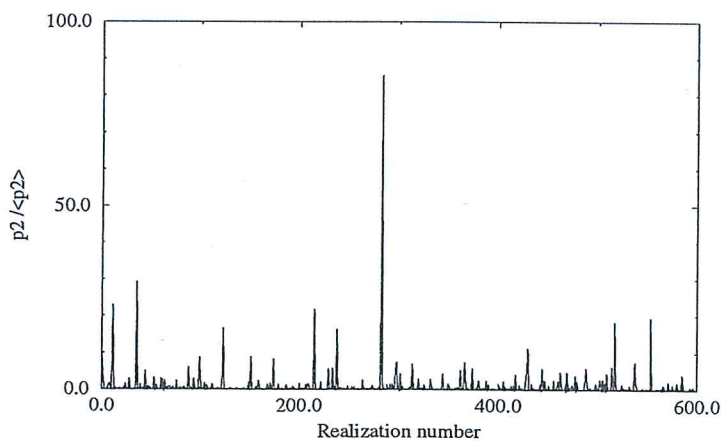


Figure 3: Normalized mean square pressure in the deep shadow zone calculated with the same parameters as considered in the experiments of Wiener and Keast ( $f = 848$  Hz,  $h_s = 3.7$  m,  $h_r = 1.5$  m,  $r \simeq 300$  m,  $\sigma = 300000$  N $\times$ m $^{-4}$  $\times$ s,  $\langle\mu^2\rangle = 2 \times 10^{-6}$ ,  $L = 1.1$  m)

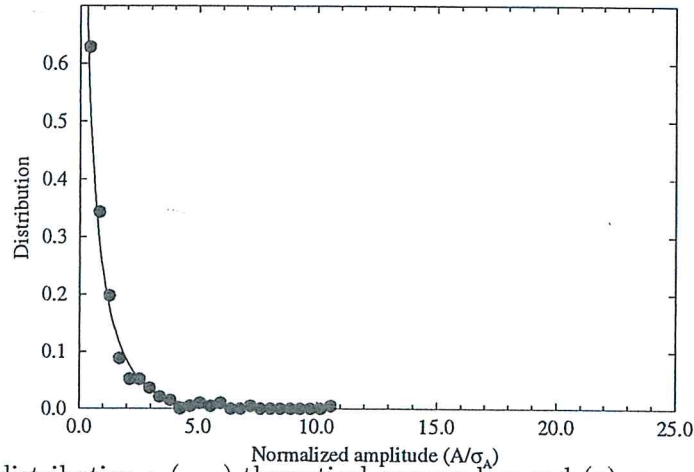


Figure 4: Amplitude distribution : (—) theoretical gamma law and (•) our computations with the same parameters as considered in the experiments of Wiener and Keast ( $f = 848$  Hz,  $h_s = 3.7$  m,  $h_r = 1.5$  m,  $r \simeq 300$  m,  $\sigma = 300000 \text{ N} \times \text{m}^{-4} \times \text{s}$ ,  $\langle \mu^2 \rangle = 2 \times 10^{-6}$ ,  $L = 1.1$  m )

can then be summarized as follows. A wide-angle parabolic wave equation in the frequency domain is used, but with coefficients depending on time. When the marching algorithm arrives at position  $x = N\Delta x$ , we simply update the random part of the index of refraction; that is, the  $u_x$  component of the velocity at point  $x$  is evaluated at the associated mean propagation time  $t = N\Delta x/c_0$  plus the emission time. It is then possible to record the time evolution of the acoustic pressure at a given location. This simple approach can be justified by an analysis of the characteristic time scales for the acoustic wave and of the turbulent field. As an example for a distance of 1500m, the transit time  $t_t$  of the acoustic wave is about 5s; the characteristic global time scale for the evolution of turbulence (eddy turn-over time) is given by  $t_g = L/u'$ , where  $L$  is the integral scale and  $u'$  the rms value of the velocity fluctuations. For atmospheric applications  $L$  and  $u'$  are in the range 1-10m and 0.1-1m/s, so that  $t_g$  and  $t_t$  are of comparable value. But it can be argued that what really matters for considering the random medium as a series of independent realizations is that  $t_g$  be large compared to the transit time through a correlation length. The ratio between the global turbulent time scale and this transit time is simply the turbulent Mach number and is therefore of order  $10^{-3}$ . For evaluation of the phase fluctuations of acoustic waves, this reasoning seems correct as they are governed by the largest turbulent structures<sup>(12)</sup>. However it is also known that the amplitude fluctuations are due to smaller turbulent structures. The time scale of these structures is given by  $t_k = 2\pi/ku'$  (Heisenberg time scale), where  $k$  is the modulus of the turbulent wave vector (the "size" of the structure is  $2\pi/k$ ). In the atmosphere, the range of values of  $k$  is very large, extending roughly from  $2\pi/L$  to  $2\pi/l_0$ ,  $l_0$  being of the order of millimeters (Kolmogorov length scale). However the very fine structures bear little energy and their role is limited by diffraction when they are much smaller than the acoustic

wavelength  $\lambda$  of interest. Taking a minimum effective scale of  $\lambda/10$ , with  $f=3400$  Hz and  $u'=1\text{m/s}$ , one obtains an estimate of the shortest "influential" turbulent time scales equal to 0.01s; during this time, an acoustic wave has travelled approximately 3m. So considering the random field as effectively time-independent for spatial steps smaller than this value for frequencies up to several kiloHertz seems very reasonable. The only remaining problem is now to generate a realistic time-evolving velocity field at a reasonable cost.

## 4.2 Large eddy simulations

The first idea is to appeal to a fluid mechanics approach. Solving the full Navier-Stokes equations is not feasible due to the extended range of turbulent structures of interest; for atmospheric studies only the Large Eddy Simulation approach (LES) seems appropriate. The basic idea in LES is to solve equations only for the largest scales of the flow, which are often most significant for the transfer of momentum or heat. Filtered Navier-Stokes equations are written for the largest turbulent scales (resolved scales), in which the smaller scales intervene due to the non-linear structure of the fluid mechanics equations. These smaller scales have to be modelled, often as an extension of the eddy viscosity concept (Lesieur<sup>9</sup>). A recent example of application of LES for air-pollution dispersion is given by Nieuwstadt *et al.*<sup>10</sup> The typical numerical grid is  $200*100*100$  points for a physical domain of size  $8\text{km}*2\text{km}*1\text{km}$ ; based on the Nyquist criterion, the minimum resolved scales are then of order 10 to 40m. We apply such an approach to the propagation of acoustic waves of frequency 1kHz in a "box" of homogeneous turbulence of dimensions  $36\text{m}*36\text{m}*200\text{m}$  with a resolution of  $23*23*160$  points (resolved scales larger than 1.5m). The computations have been done using a finite-volume code (TRIO-VF). As an initial condition, a velocity field having an r.m.s. magnitude of  $3\text{m/s}$  and integral scale of  $5\text{m}$  was generated using the techniques described in section 3.1. This field was evolved in time for approximately 4 eddy turnover times (based on the initial conditions) to allow the artificial structures introduced by the initial field to be replaced by those governed by the Navier-Stokes equation (see Fig. 5). At this point the r.m.s. velocity had reached  $1\text{m/s}$ , and the acoustic calculation commenced.

Acoustic computations have been done with a wide-angle 3D parabolic equation code based on the split-step Fourier algorithm first described by Thomson and Chapman<sup>5</sup>; the FFT was done on a  $256*256$  points grid ( $\Delta y = \Delta z = .14\text{m}$ , ie 2.5 points per wavelength) with a marching step of  $\Delta x = 2\text{m}$ . The source consisted of a plane wave of unit amplitude and  $1\text{kHz}$  frequency introduced at the end ( $x = 0$ ) of the "box". Results are shown in Fig. 6 for the amplitude of the acoustic pressure in a plane located at 200m from the source. The two plots are snapshots taken at two times separated by 4.7s.

Large blobs of amplified or rarefied sound are visible, but no fine structure of the field is apparent (say for dimensions less than 1m). The two plots display significant differences, but the time-evolution of the received pressure at a given location (not shown) proved disappointing. Only very slow variations were present; in fact the characteristic time scale of the smaller resolved eddies is about 1.5s, and this appears to be far too large a value for acoustics; the problem being that we have no acoustic modelling for the role of the smaller turbulent structures. Of course it is possible to increase the

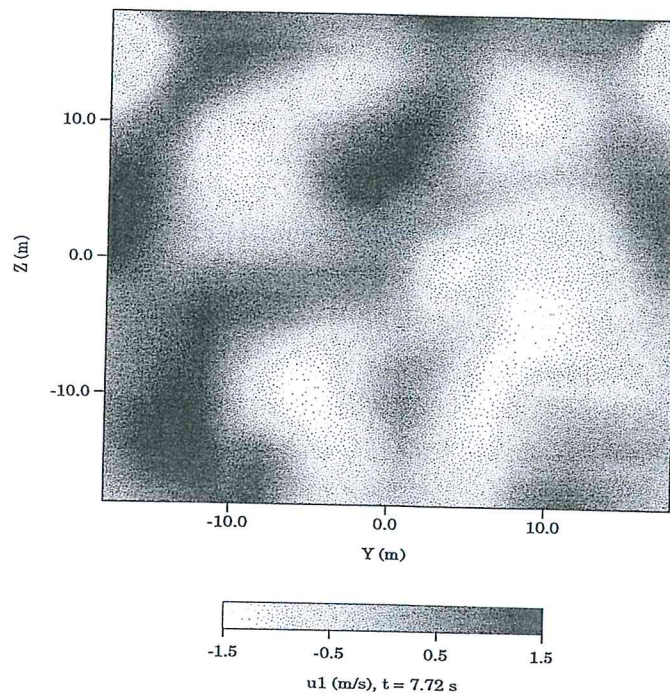


Figure 5: One instant in time of the velocity component in the direction of propagation,  $u_x$ , obtained from the LES simulation. A plane perpendicular to the propagation direction is depicted.

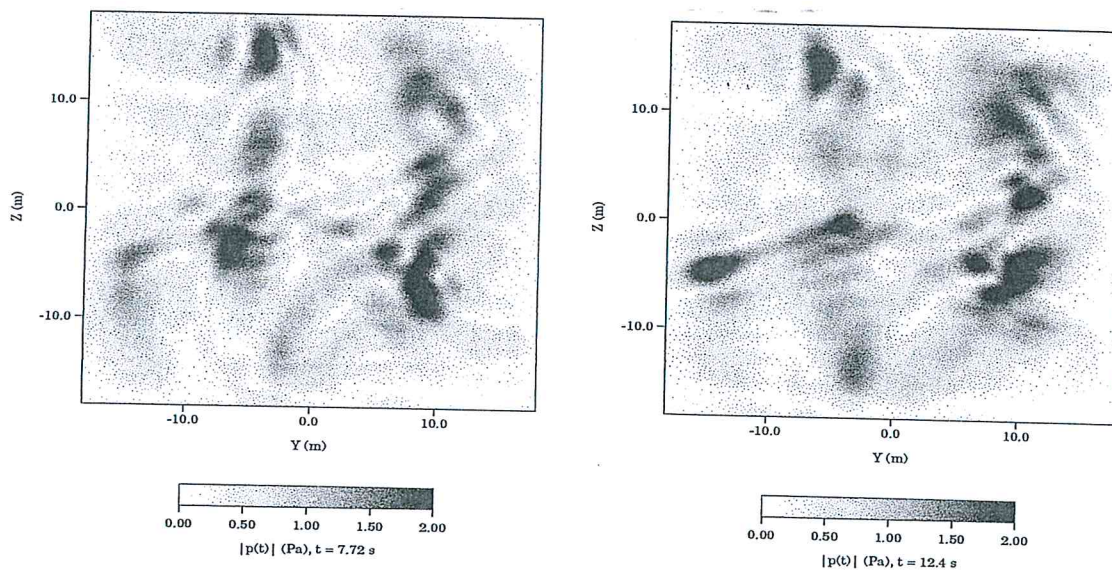


Figure 6: Instantaneous pressure amplitudes in a plane perpendicular to the direction of the incident acoustic wave and using the LES derived velocity field.



spatial resolution of the LES code (the number of grid points being around  $10^5$ ); but for acceptable computation times the number of points in each direction can at most be increased by a factor of 3. This seems to be too small for describing a significant part of the inertial range of the turbulent spectrum; and the problem would be even more dramatic if full scale application would be considered. So we turned to a different approach, based on an extension of the Fourier modes technique described above.

### 4.3 Time-evolving Fourier modes

The basic idea is to add a time dependence to the static Fourier modes described in section 3. Following Bailly *et al* <sup>(1)</sup> (see also Drummond *et al* <sup>(14)</sup>), we simulate the velocity at point  $\mathbf{x}$  as:

$$\mathbf{u}(\mathbf{x}, t) = \sum_{n=1}^N \tilde{u}_n \cos[\mathbf{k}_n \cdot (\mathbf{x} - t\mathbf{U}_c) + \psi_n + \omega_n t] \boldsymbol{\sigma}_n \quad (7)$$

Because of the fluid incompressibility  $\mathbf{k}_n$  is normal to its associated Fourier contribution  $\tilde{\mathbf{u}}_n$ . The field isotropy in 3D requires that the directions of  $\mathbf{k}_n$  and  $\tilde{\mathbf{u}}_n$  have the following p.d.f. :

$$P(\phi) = \frac{1}{\pi} \quad P(\theta) = \frac{1}{2} \sin \theta \quad P(\alpha) = \frac{1}{2\pi} \quad (8)$$

with  $0 \leq \theta \leq \pi$ ,  $0 \leq \phi \leq \pi$  and  $0 \leq \alpha \leq 2\pi$ . The field homogeneity is obtained by selecting  $\psi$  from a uniform p.d.f. between 0 and  $2\pi$ . The modulus of  $\tilde{\mathbf{u}}_n$  is such that:

$$\tilde{u}_n = \sqrt{E(k_n) \Delta k_n} \quad \text{with} \quad k_n = |\mathbf{k}_n| \quad (9)$$

$E(k_n)$  is the 3D kinetic energy spectrum, which is approximated by a von Karman expression:

$$E(k) = \mathcal{A} \frac{\overline{u^2}}{k_e} \frac{(k/k_e)^4}{[1 + (k/k_e)^2]^{17/6}} \exp \left[ -2 \left( \frac{k}{k_\eta} \right)^2 \right] \quad (10)$$

where  $k_\eta$  is the Kolmogorov length scale. The two parameters  $\mathcal{A}$  and  $k_e$  are adjusted so as to give the desired total energy and integral length scale. We consider a temporal evolution of each mode governed by a circular frequency  $\omega_n$ . This frequency is a random variable whose mean value is related to the turbulent wave number through the Heisenberg formula:  $\omega_o = k * u'$ ; the pdf of  $\omega_n$  is chosen as a Gaussian according to:

$$g(\omega) = \frac{1}{\omega_o \sqrt{2\pi}} \exp \left( -\frac{(\omega - \omega_o)^2}{2\omega_o^2} \right) \quad (11)$$

This synthetic turbulence model has been successfully applied to the study of the generation of noise by turbulent flows <sup>(1)</sup>. In Fig. 7 we have plotted the spatial evolution of the "effective" component of the velocity fluctuation  $u_x$ , computed with the time-evolving Fourier modes.

The integral scale is 5m (corresponding wavenumber equals to 1.25), the r.m.s. value of the velocity fluctuations is 1m/s; 100 modes have been distributed between  $k_{min}=1$  and  $k_{max}=10$ . Comparison with the LES results (see Fig. 5) reveals that much smaller turbulent structures can be represented

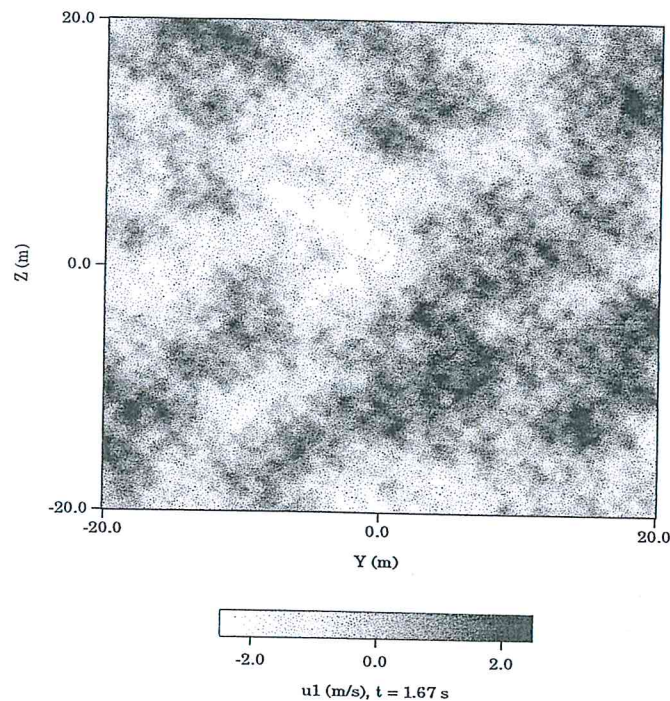


Figure 7: One instant in time of the velocity component in the direction of propagation  $u_x$  obtained using the time-evolving random Fourier modes model. A plane perpendicular to the direction of the acoustic wave propagation is depicted.

in this way. The amplitude of pressure fluctuations, obtained for the same conditions used in the LES computations are shown (save for the marching step:  $\Delta x = 1m$ ), in Fig. 8 for four values of the observation time. Consecutive snapshots are separated by 1.2s. It is clear that, in reference to the LES results (Fig. 5) fluctuations of smaller spatial scales are now visible.

However, it can be noted that the differences between LES and RFM are less striking for the acoustic field than for the velocity field. A sort of filtering effect takes place, so that there is very low acoustic energy for structures smaller than around 1m. As a final result we display on Fig. 9 the time evolution of the normalized squared pressure at a point located at the end of the computational domain ( $x=200m$ ). The computation has been done for 128 points with a time step of 80ms. Even if the sample is relatively short compared to the characteristic time scales of the turbulence field (eddy turn-over time equals to 5s), this plot demonstrates the large variability of the amplitude of the received signal: Periods of high intensity alternate with other periods where the amplitude is near zero. The frequency spectrum of the amplitude fluctuations ( Fig. 10 ), averaged over the plane at  $x=200m$ , shows that most of the energy is concentrated in the low frequencies (below 1Hz); for the highest frequencies, a power law is apparent with a variation in  $f^{-5/3}$ .

## 5 Conclusion

In this paper we have presented a first approach to the numerical simulation of the propagation of acoustic waves through time-dependent random media. Two methods for generating the random index

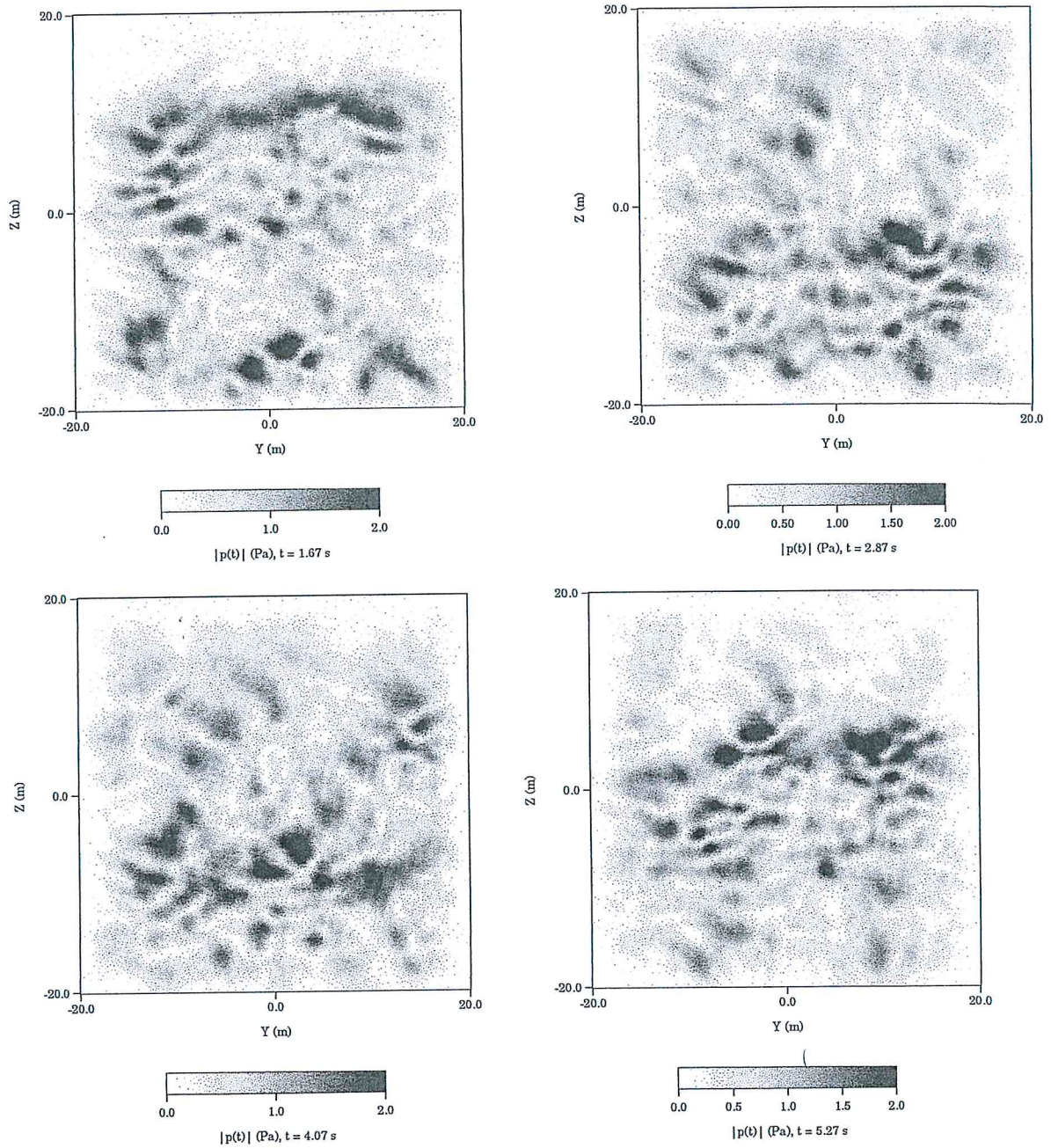


Figure 8: Instantaneous pressure amplitudes in a plane perpendicular to the direction of the incident ( $x=200\text{m}$ ) acoustic wave and using the time-evolving Fourier modes

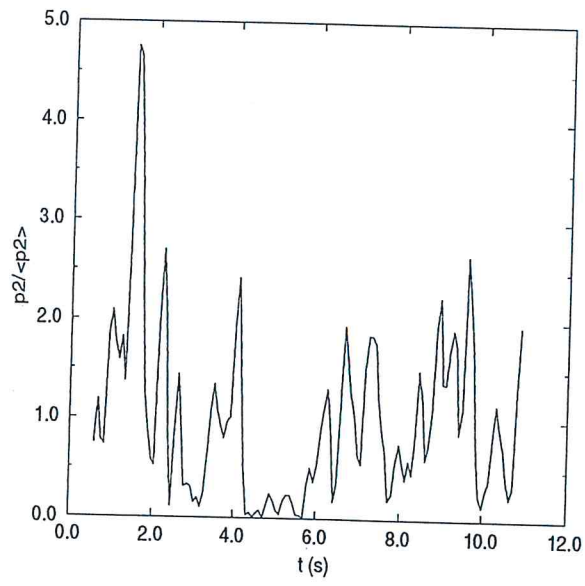


Figure 9: Normalized square pressure as a function of time.

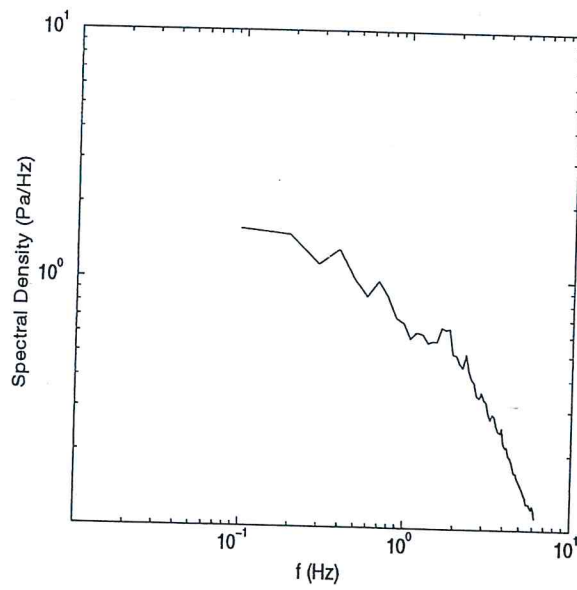


Figure 10: Spectral density of the pressure amplitude.

of refraction field have been considered: Large Eddy Simulations and an extension of the Random Fourier Modes method. The LES approach suffers from a resolution limitation, as small turbulent structures, in the inertial range zone of the spectrum, seem to play an important role in determining the amplitude fluctuations of the sound waves. A parametric study, using RFM, of the importance of spatial-frequency cut-off of the turbulent field will allow us to make clear what resolution is really needed for atmospheric propagation studies and if the LES approach is viable.

## Acknowledgment

Support for K. Wert was provided by a Chateaubriand Fellowship awarded by the government of France.

## References

- <sup>1</sup>C. Bailly, Ph. Lafon, S. Candel. A stochastic approach to compute noise generation and radiation of free turbulent flow. 16th AIAA Aeroacoustic Conference, Munich, Germany, CEAS-AIAA paper n° 95-092, 1995.
- <sup>2</sup>Ph. Blanc-Benon, D. Juvé, and G. Comte-Bellot. Occurrence of caustics for high-frequency acoustics waves propagating through turbulent fields. *Theoret. Comput. Fluid Dynamics*, 2:271-278, 1991.
- <sup>3</sup>Y. Hugon-Jeannin. *Simulation numérique de la propagation d'ondes acoustiques en milieu turbulent*. PhD thesis, Ecole Centrale de Lyon, 1992. n° 92-37.
- <sup>4</sup>M. Karweit, Ph. Blanc-Benon, D. Juvé, and G. Comte-Bellot. Simulation of the propagation of an acoustic wave through a turbulent velocity field: a study of phase variance. *J. Acoust. Soc. Am.*, 89:52-62, 1991.
- <sup>5</sup>D. J. Thomson and N. R. Chapman. A wide angle split-step algorithm for the parabolic equation. *J. Acoust. Soc. Am.*, 74:1848-1854, 1983.
- <sup>6</sup>P. Chevret, Ph. Blanc-Benon, and D. Juvé. A numerical model for sound propagation through a turbulent atmosphere near the ground. *J. Acoust. Soc. Am.*, 100:3587-3599, 1996.
- <sup>7</sup>K. E. Gilbert, R. Raspet, and X. Di. Calculation of turbulence effects in an upward-refracting atmosphere. *J. Acoust. Soc. Am.*, 87:2428-2437, 1990.
- <sup>8</sup>D. Juvé, Ph. Blanc-Benon, and G. Comte-Bellot. Transmission of acoustic waves through mixing layers and 2d isotropic turbulence. In *Turbulence and coherent structures*, pages 367-384. O. Métais and M. Lesieur eds., Kluwer, Boston, 1990.
- <sup>9</sup>M. Lesieur. Recent approaches in large-eddy simulations of turbulence. In *New Tools in Turbulence Modelling* pages 1-28. O. Métais and J. Fertziger, eds, Les Editions de Physique, Springer, Kluwer, Paris, 1997.
- <sup>10</sup>F. T. M. Nieuwstadt and J. P. Meeder. *Large-eddy simulation of air pollution dispersion: a review*. In *New Tools in Turbulence Modelling* pages 265-279. O. Métais and J. Fertziger, eds, Les Editions de Physique, Springer, Kluwer, Paris, 1997.
- <sup>11</sup>D. Juvé, Ph. Blanc-Benon, and P. Chevret. *Sound propagation through a turbulent atmosphere: influence of the turbulence model*. In *Proceedings of the Sixth International Symposium on Long Range Sound Propagation*, pages 270-282, Ottawa, June 1994, Canada.
- <sup>12</sup>V. I. Tatarskii. *The effect of a turbulent atmosphere on wave propagation*. I.P.S.T Keter Press, Jerusalem, 1971.
- <sup>13</sup>D. I. Havelock, M. R. Stinson, and G. A. Daigle. *Aspects of sound field fluctuations in a refractive shadow*. In *Proceedings of the Sixth International Symposium on Long Range Sound Propagation*, pages 152-166, Ottawa, June 1994. Canada.
- <sup>14</sup>I. T. Drummond and S. Duane, and R. R. Horgan. Scalar diffusion in simulated helical turbulence with molecular diffusivity. *J. Fluid Mech.*, 138:75-91, 1984.
- <sup>15</sup>R. H. Kraichnan. Diffusion by a random velocity field. *Phys. Fluids*, 13(1):22-31, 1970.
- <sup>16</sup>F. M. Wiener and D. N. Keast. Experimental study of the propagation of sound over ground. *J. Acoust. Soc. Am.*, 31:724-733, 1959.